A Kinetic Study on Nickel Electrodeposition from Sulfate Acid Solutions : II. Reaction Modeling

Ana Isabel C. Santana, Susana L. Díaz, Oswaldo E. Barcia and Oscar R. Mattos

J. Electrochem. Soc. 2009, Volume 156, Issue 8, Pages D331-D335.
doi: 10.1149/1.3151686

Journal of The Electrochemical Society, **156** (8) D331-D335 (2009)
0013-4651/2009/156(8)/D331/5/$25.00 © The Electrochemical Society

A Kinetic Study on Nickel Electrodeposition from Sulfate Acid Solutions

II. Reaction Modeling

Ana Isabel C. Santana,[a] Susana L. Díaz,[a] Oswaldo E. Barcia,[a,b] and Oscar R. Mattos[a,*,z]

[a]*Laboratório de Ensaios Não-Destrutivos, Corrosão e Soldagem, Departamento e Programa de Engenharia Metalúrgica e de Materiais, and* [b]*Instituto de Química, Universidade Federal do Rio de Janeiro, 21941-972, Rio de Janeiro, Brazil*

The electrochemical mechanism of Ni electrodeposition in an acid sulfate medium with pH ranging from 1 to 6 is evaluated. For pH ≤ 3, a reaction model already available in the literature accounts satisfactorily for the experimental results shown in Part I of the present paper. However, this model cannot explain the results obtained in the pH interval of 4–6. A complementary model is then proposed, considering the formation of two species: (*i*) $[Ni(OH)]^{+}_{ads}$, the relaxation of which is associated with a capacitive loop at medium frequencies, and (*ii*) $[Ni(OH)]_{ads}$, the relaxation of which gives rise to an inductive loop at low frequencies. The validation of this model has been accomplished by the comparison with the experimental polarization curves and impedance measurements. A good agreement is found between the simulated and experimental results. By using the previous model proposed by Epelboin et al. [*J. Electroanal. Chem.*, **119**, 61 (1981)] for pH ≤ 3 together with the present complementary model, Ni electrodeposition can now be explained in the whole pH range of 1–6.
 [DOI: 10.1149/1.3151686]

Manuscript submitted January 30, 2009; revised manuscript received May 14, 2009. Published June 22, 2009.

In Part I of this paper, the kinetics of Ni electrodeposition in acid sulfate solutions, with the pH ranging from 1 to 6, was analyzed by polarization curves, ac impedance spectroscopy, and interfacial pH measurements.[1] A summary of the most important experimental results can be outlined as follows.

The cathodic polarization curves obtained in the solution at the pH interval of 1–3 showed a behavior similar to that reported by Epelboin et al.[2] for Ni sulfate solutions at pH 1.5 and 3. The increase in pH caused a shift to more negative potentials in the so-called part 2[1] of the curves, wherein Ni electrodeposition occurs with high efficiency. For the curves obtained in the pH interval of 4–6, an opposite shift was detected.

The impedance diagrams taken at the pH range of 1–3 showed, in conformity with the results of Epelboin et al.,[2] an inductive loop that was associated with the $Ni(I)_{ads}$ intermediate, followed by a capacitive one in the low frequency domain, related to a blocking effect of hydrogen at the electrode surface. However, at high polarizations at pH 3, a transition in this behavior was verified. In such conditions, the inductive–capacitive behavior was replaced by a capacitive loop followed by an inductive one. As previously discussed,[1] this inversion cannot be explained by the model of Epelboin et al.[2] Moreover, on diagrams obtained in the pH interval of 4–6, the same behavior was detected. The capacitive loop at medium frequencies (0.5–5.8 Hz) was associated with $[Ni(OH)]^{+}_{ads}$, whose relaxation was pH dependent. In turn, the inductive loop at around 0.02 Hz was proposed to be related to the $[Ni(OH)]_{ads}$ relaxation. Interfacial pH measurements revealed the existence of local alkalination during Ni electrodeposition within the whole pH range investigated. At pH 3, the transition from the inductive–capacitive behavior to a capacitive–inductive one detected by the impedance diagrams was always associated with a significant increase in the interfacial pH. Indeed, in the pH interval of 4–6, the high efficiency in Ni electrodeposition (part 2 of the polarization curves) only began when the interface alkalination reached pH 6. In this condition, a capacitive–inductive behavior was always evident in the corresponding impedance diagrams.

In this Part II of the paper, the proposed reaction path for Ni electrodeposition within the pH interval of 4–6 is expounded and transcribed into mathematical expressions aiming at the simulation of the experimental results presented in Part I of this paper.[1] This reaction path, together with the one proposed by Epelboin et al.,[2] is capable to explain the results for Ni electrodeposition in sulfate acid solutions in the whole pH interval of 1–6. The entire reaction model that describes the process over such a large pH range is valuable for further studies, especially those related to Ni alloy electrodepositon.

Reaction Model

During Ni electrodeposition from sulfate acid solutions, the cationic reactive species should be Ni^{2+}, Ni^{+}, and H^{+}. Intermediate species, probably of the hydroxylated type, can also be considered. Charge transfer in multiple steps might take place at the electrode surface through adsorbed intermediates, which can interact with other inhibiting species.[3] This gives rise to relaxation processes that strongly depend on the electrolyte composition, pH, nature of the anion, polarization, and hydrodynamic conditions.[4] It has been well known that the processes of nucleation and growth during electrodeposition of metals can generate relatively distorted loops in complex plane impedance diagrams.[4,5] Accordingly, during Ni electrodeposition from sulfate solutions, surface interactions between Ni^{2+} and H^{+} have been reported.[2,6] These interactions, in conjunction with the anion influence, were considered to describe the electrochemical impedance results. The interpretation of the experimental data was done in terms of adsorbed intermediates as well as of the potential dependence of growth sites.[2,6]

As already mentioned, the model proposed by Epelboin et al.[2] for Ni electrodeposition satisfactorily describes the experimental results on Ni electrodeposition from sulfate solutions at pH 1.5 and 3. However, the existence of two trends in the steady-state polarization curves as well as the change in the nature of impedance diagrams were detected with pH ranging from 1 to 6.[1] An unambiguous transition in the mechanism of Ni electrodeposition was observed beginning at high polarizations in pH 3.[1] Such dissimilar behavior remains the same up to pH ≈ 6. Because this change cannot be described by the earlier proposed model,[2,6] a complementary reaction path is now put forward, aiming to describe the experimental results in the pH interval of 4–6. In this model, the formation of two distinct species, $[Ni(OH)]^{+}_{ads}$ and $[Ni(OH)]_{ads}$, can be written as

$$Ni^{2+} + H_2O + e \underset{k_1}{\overset{k_{-1}}{\rightleftarrows}} [Ni(OH)]^{+}_{ads} + H \qquad [1]$$

* Electrochemical Society Active Member.
z E-mail: omattos@metalmat.ufrj.br

$$[Ni(OH)]^{+}_{ads} + Ni^{2+} + 2e \xrightarrow{k_{-2}} [Ni(OH)]^{+}_{ads} + Ni \quad [2]$$

$$[Ni(OH)]^{+}_{ads} + e \underset{k_3}{\overset{k_{-3}}{\rightleftarrows}} [Ni(OH)]_{ads} \quad [3]$$

$$[Ni(OH)]_{ads} + Ni^{2+} + 2e \xrightarrow{k_{-4}} [Ni(OH)]_{ads} + Ni \quad [4]$$

Reaction 1 corresponds to the generation of $[Ni(OH)]^{+}_{ads}$, which acts as a catalyst for Ni electrodeposition in Reaction 2 or can be converted into $[Ni(OH)]_{ads}$ species through Reaction 3. It is important to point out that if Reactions 1 and 3 were considered as irreversible, i.e., $k_1 = k_3 = 0$, it is not possible to observe both the inductive and the capacitive loops during the simulation process. This is the reason for the assumption of Reactions 1 and 3 being reversible paths.[7,8] The species $[Ni(OH)]_{ads}$ may also catalyze Ni electrodeposition via Reaction 4. Hence, k_{-2} and k_{-4} were associated with autocatalytic reactions and were not included in the mass balance calculation. Consequently, the relaxation frequency of these two adsorbed species are not current dependent.[7,8]

The following assumptions were adopted:

1. The high frequency capacitive loop in the impedance plots is related to the double-layer capacitance, C_{dl}, in parallel with the charge-transfer resistance, R_t. The values of C_{dl} were taken from the experimental plots[1] being, in average, 75 μF cm^{-2}. This value was kept constant during the simulation.
2. For electrochemical reactions, the rate constants vary with the potential, E, according to Tafel's law

$$k_{-i} = k_{0-i}e^{(-b-iE)}; \quad b_{-i} = \frac{\alpha_i F}{RT}$$

and

$$k_i = k_{0i}e^{(biE)}; \quad b_i = \frac{(1-\alpha_i)F}{RT}$$

where k_i and k_{-i} are potential-dependent parameters; k_{0i} and k_{0-i} comprise the corresponding rate constant as well as the concentration of reactive species; b_i and b_{-i} are activation coefficients with values between 0 and 38.4 V^{-1}, corresponding to α_i varying between 0 and 1 for one-electron transfer.
3. The Langmuir isotherm is considered valid for the adsorption processes because it does not introduce additional constants to be adjusted in the model. By using this procedure, an accurate evaluation of the reaction path is possible. In this case, θ_i is the potential- and time-dependent parameter. Therefore, θ_1 corresponds to the surface fraction covered by $[Ni(OH)]^{+}_{ads}$ species, θ_2 represents the surface coverage by $[Ni(OH)]_{ads}$ species, and $(1 - \theta_1 - \theta_2)$ is the electrode free surface.
4. No constant-phase element was assumed and, therefore, no fitting procedure was done. Only a trial and error simulation procedure was adopted.

Based on these hypotheses, the charge balance gives the total current that flows through the electrode interface

$$\frac{I}{F} = -k_{-1}(1-\theta_1-\theta_2) + k_1\theta_1 - 2k_{-2}\theta_1 - k_{-3}\theta_1 + k_3\theta_2 - 2k_{-4}\theta_2 \quad [5]$$

The mass balances for the two adsorbed species are given by

$$\beta_1\frac{\partial\theta_1}{\partial t} = k_{-1}(1-\theta_1-\theta_2) - k_1\theta_1 - k_{-3}\theta_1 + k_3\theta_2 \quad [6]$$

$$\beta_2\frac{\partial\theta_2}{\partial t} = k_{-3}\theta_1 - k_3\theta_2 \quad [7]$$

where β_1 and β_2 denote the maximal surface concentration of the respective adsorbed species on the electrode surface, expressed in mol cm^{-2}. In this paper, adopting the widely accepted value for iron-group metals,[2-8] β_i was taken as 10^{-8} mol cm^{-2} and corresponds to about one monolayer for one intermediate bonding to one surface metal atom.

Steady state.— In the steady-state condition, the surface coverage is considered constant with time, i.e., $\partial\theta_1/\partial t = \partial\theta_2/\partial t = 0$. Therefore, the steady-state values for θ_i can be calculated as

$$\overline{\theta_1} = \frac{k_{-1}k_3}{X} \quad [8]$$

$$\overline{\theta_2} = \frac{k_{-1}k_{-3}}{X} \quad [9]$$

$$1 - \overline{\theta_1} - \overline{\theta_2} = \frac{k_1k_3}{X} \quad [10]$$

where $X = k_{-1}k_3 + k_1k_3 + k_{-1}k_{-3}$.

The stationary current can be obtained from Eq. 5-7 and expressed by

$$\overline{I} = -2F(k_{-2}\overline{\theta_1} + k_{-4}\overline{\theta_2}) \quad [11]$$

The steady-state polarization curves can thus be simulated according to Eq. 8-11, with suitable values for k_{0i} and b_i.

Electrode impedance.— The faradaic impedance Z_F can be calculated by linearizing Eq. 5-7

$$\frac{1}{Z_F} = \frac{1}{R_t} - F[(-k_{-1} - k_1 + 2k_{-2} + k_{-3})\Delta\theta_1 + (-k_{-1} - k_3 + 2k_{-4})\Delta\theta_2] \quad [12]$$

where R_t is the charge-transfer resistance defined by

$$R_t = \lim_{\varpi\to\infty} Z_F$$

and given by

$$\frac{1}{R_t} = F[(38.4k_1 + 2b_{-2}k_{-2})\overline{\theta_1} + (38.4k_3 + 2b_{-4}k_{-4})\overline{\theta_2}] \quad [13]$$

with $\overline{\theta_1}$ and $\overline{\theta_2}$ being the steady-state values. The relaxation of θ_i due to a small amplitude sine wave potential perturbation can be derived from Eq. 6 and 7

$$\Delta\theta_1 = \frac{\partial\theta_1}{\partial E} = \frac{\{38.4[Z_2(k_3\overline{\theta_2} - k_1\overline{\theta_1}) + k_3\overline{\theta_2}(k_{-1} - k_3)]\}}{Z_1Z_2 + k_{-3}(k_{-1} - k_3)} \quad [14]$$

$$\Delta\theta_2 = \frac{\partial\theta_2}{\partial E} = \frac{-38.4k_3\overline{\theta_2} + k_{-3}\Delta\theta_1}{Z_2} \quad [15]$$

where

$$Z_1 = k_{-1} + k_1 + k_3 + j\omega\beta_1$$

$$Z_2 = k_3 + j\omega\beta_2$$

Once k_{0i} and b_i are determined, Eq. 14 and 15 allow the calculation of $\partial\theta_i/\partial E$. By substituting these values in Eq. 12, the faradaic impedance is obtained. From this calculus and considering the relative predominance of $[Ni(OH)]^{+}_{ads}$ and $[Ni(OH)]_{ads}$, the relaxation of the corresponding θ_1 and θ_2 gives rise to capacitive and inductive loops, respectively.[7-9] Finally, the electrode impedance can be numerically simulated considering the double-layer capacitance C_{dl} in parallel with Z_F. As already mentioned, the value of C_{dl} was taken as 75 μF cm^{-2}, the experimental average value. The number of pa-

Table I. Rate constant values, k_{0i}, used on the simulation calculations of both the steady-state polarization curves and impedance diagrams in the pH interval of 4–6.

k_{0i} (s^{-1})	pH 4	pH 5	pH 6
k_{01}	4.0×10^{1}	0.6×10^{1}	0.6×10^{1}
k_{0-1}	2.0×10^{-20}	9.3×10^{-20}	3.0×10^{-19}
k_{0-2}	1.5×10^{-25}	8.0×10^{-24}	9.0×10^{-24}
k_{03}	0.2×10^{1}	0.3×10^{1}	0.3×10^{1}
k_{0-3}	2.5×10^{-19}	3.1×10^{-19}	3.5×10^{-18}
k_{0-4}	2.3×10^{-17}	9.6×10^{-17}	6.0×10^{-16}

rameters to be adjusted does not allow a fitting procedure. Moreover, the fitting would require at least three phase constant elements to be adjusted.

Simulation and Discussion

The parameters used to simulate the experimental results on Ni electrodeposition from the acid sulfate solution within the pH interval of 4–6 are given in Tables I and II. The results of the simulation of the steady-state polarization curves in this pH range are shown in Fig. 1. This figure, in which the experimental data are also presented, provides evidence of the good agreement between the calculated and the experimental steady-state results. The main parameters for the simulation of the polarization curves were k_{-2} and k_{-4}. Indeed, the parameters in Table I show that an increase in k_{-4} and k_{-2} causes an intensification of the steady-state currents. By keeping b_{-2} and b_{-4} values independent of pH, only k_{0-2} and k_{0-4} were adjusted to simulate the pH effects. Accordingly, in Fig. 1 the simulation of

Table II. Activation coefficient values, b_i, used on the calculations of both the steady-state polarization curves and impedance diagrams in the pH interval of 4–6.

b_i (V^{-1})	pH 4	pH 5	pH 6
b_1	16.0	15.9	14.6
b_{-1}	22.4	22.5	23.8
b_{-2}	31.0	31.0	31.0
b_3	19.4	19.4	19.4
b_{-3}	19.0	19.0	19.0
b_{-4}	16.0	16.0	16.0

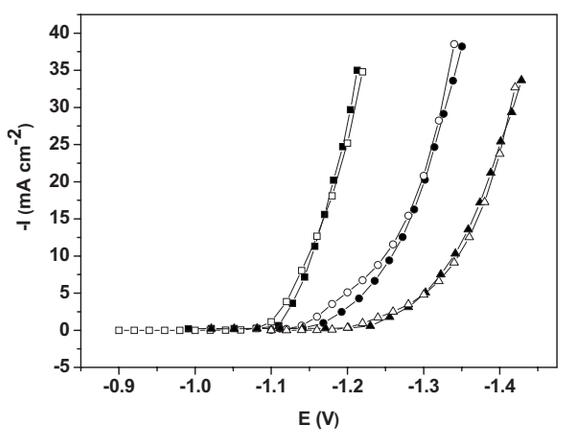

Figure 1. Steady-state cathodic polarization curves obtained in the 1.2 M $NiSO_4 \cdot 6H_2O$ solution at different pH values: (■) 6, (●) 5, and (▲) 4 experimental results; (□) 6, (○) 5, and (△) 4 simulated results.

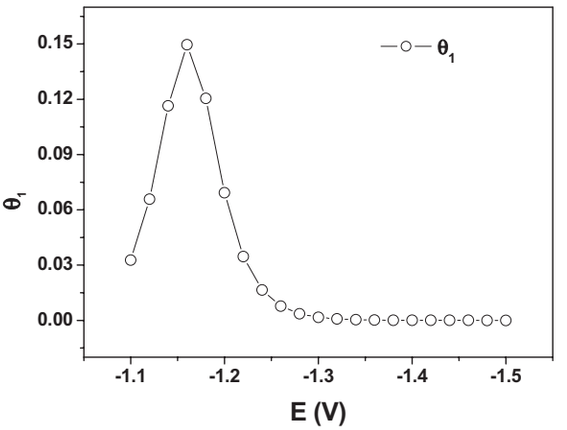

Figure 2. Potential dependence of θ_1 for the 1.2 M $NiSO_4 \cdot 6H_2O$ solution at pH 5, calculated by means of the set of parameters in Tables I and II.

the pH increase reproduces the shift in part 2 of the curves toward more positive potentials,[1] namely, an activation of the metallic deposition, in conformity with the experimental data.

The activation effect on the deposition process due to a pH increase is justified by the difference in the rates of forward and backward directions in Reaction 1 of the model. Indeed, the higher the pH, the higher the concentration of $[Ni(OH)]^{+}_{ads}$ at the electrode surface. From Table I, it is clear that the k_{-1} value increases with increasing pH and should affect k_{-2} in Reaction 2. The $[Ni(OH)]^{+}_{ads}$ species can also generate an intermediate, $[Ni(OH)]_{ads}$, which is associated with k_{-4}. Because the simulation of part 2 of the polarization curves is strongly affected by the value of k_{-4}, it is assumed that $[Ni(OH)]_{ads}$ should prevail in this potential range.

From the potential dependence of the electrode coverages θ_1 and θ_2 calculated for pH 5 and depicted, respectively, in Fig. 2 and 3, there is an enhancement of both processes with increasing cathodic polarization. However, θ_1 presents a maximum near −1.15 V and then starts to decrease abruptly, attaining a value near zero at higher polarizations. Conversely, θ_2 does not show any decline, remaining at high levels throughout high negative potentials. The potential value associated with the maximum of θ_1 corresponds to the beginning of part 2 of the polarization curve. This fact confirms the predominance of the surface coverage by $[Ni(OH)]_{ads}$ throughout part 2 of the polarization curve. Such qualitative behavior was found to be similar in the whole pH range investigated in this work.

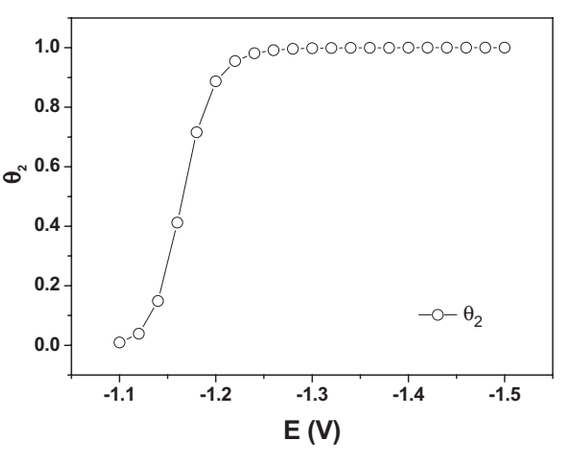

Figure 3. Potential dependence of θ_2 for the 1.2 M $NiSO_4 \cdot 6H_2O$ solution at pH 5, calculated by means of the set of parameters in Tables I and II.

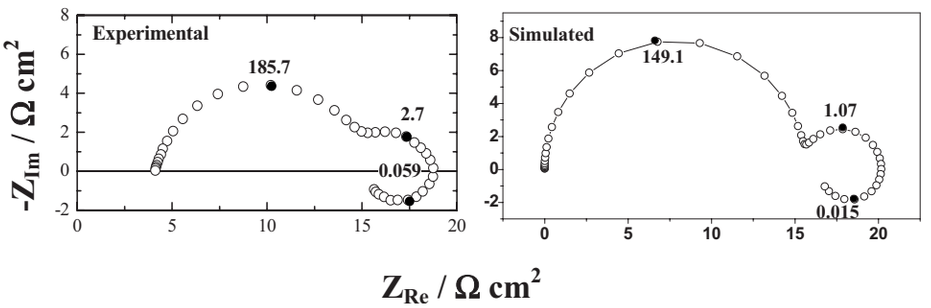

Figure 4. Simulated and experimental diagrams obtained in the 1.2 M $NiSO_4 \cdot 6H_2O$ solution at pH 5 and $E = -1.15$ V (frequencies in hertz).

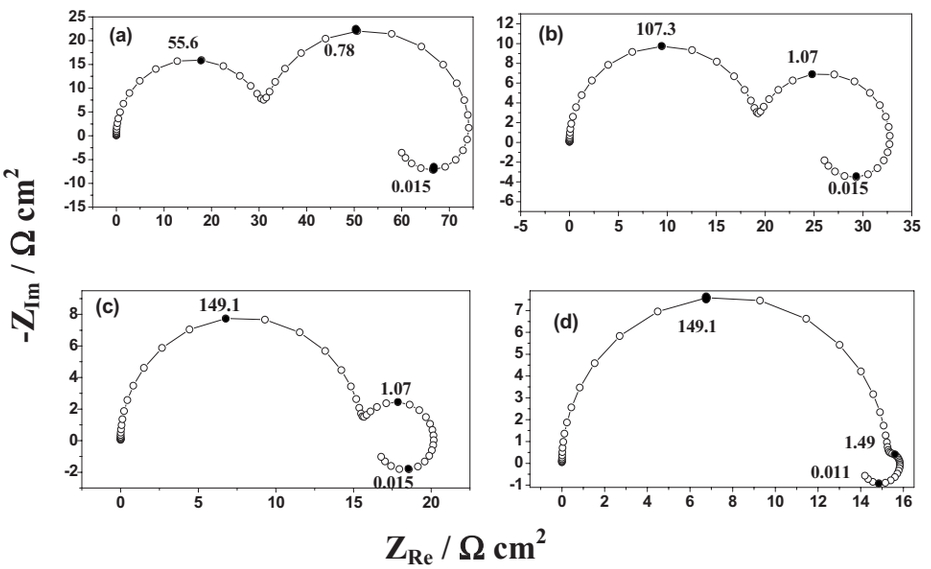

Figure 5. Simulated diagrams for 1.2 M $NiSO_4 \cdot 6H_2O$ solution, pH 5, at different potential values: (a) −1.13, (b) −1.14, (c) −1.15, and (d) −1.16 V (frequencies in hertz).

By using the same set of parameters applied to the calculation of the polarization curves (Tables I and II), the impedance diagrams for Ni electrodeposition in sulfate solution at pH 5 were simulated and shown in Fig. 4 and 5. In all calculated plots, as in the experimental ones,[1] the high frequency capacitive loop corresponds to the double-layer capacitance in parallel with charge-transfer resistance, R_t. This feature is followed, in the low frequency domain, by a capacitive loop at medium frequencies that mainly corresponds to the relaxation of $\theta_1(\partial\theta_1/\partial E)$ and by an inductive loop, which is related to the relaxation of $\theta_2(\partial\theta_2/\partial E)$. The simulated results agree with the experimental data.[1] The parameters proposed by the trial and error procedure, shown in Tables I and II, were obtained by a compromise between the quality of simulation results of both steady-state polarization curves and impedance diagrams.

Figure 4 shows a comparison between the experimental and simulated diagrams obtained at the same potential value ($E = -1.15$ V) and at pH 5. The quantitative results of this evaluation are presented in Table III. In this table, the experimental and calculated values for R_p and R_t are rather close, and the corresponding frequencies of the three loops agree with each other.

Table III. Resistance and frequency values taken from the experimental and simulated diagrams in Fig. 4.

	R_t (Ω cm^2)	R_p (Ω cm^2)	f_1 (Hz)	f_2 (Hz)	f_3 (Hz)
Experimental	15.0	15.7	185.7	2.7	5.2×10^{-2}
Simulated	15.6	16.5	149.1	1.1	1.5×10^{-2}

The potential dependence was also determined, as shown in Fig. 5. The decrease with increasing cathodic polarization of both values of the charge-transfer resistance R_t and polarization resistance R_p was simulated in accordance with the experimental data. The experimental R_p data were obtained from the compromise between the values taken from both impedance diagrams and polarization curves by means of graphical adjustment. Moreover, the capacitive loop at medium frequencies decreases in size with increasing polarization, as it was verified from the experimental plots.[1] Because this loop was attributed to $\partial\theta_1/\partial E$, this aspect also conforms to the behavior depicted in Fig. 2, i.e., the diminution of the $[Ni(OH)]^+_{ads}$ coverage of the electrode surface at higher polarizations. The inductive loop remains fairly constant with increasing potential, also in accordance with the experimental data.[1]

The concordance of the model with the experimental data also comprises the pH effect, as illustrated in the diagrams of Fig. 6 for the same potential value. In these diagrams, the frequency of the capacitive loop associated with $\partial\theta_1/\partial E$ is pH dependent. By simulating the pH increase, this loop tends to be more noticeable. As verified from the calculated polarization curves (Fig. 1), when k_{-4} and k_{-2} augment (Table I), a shift to more positive potentials and a current increase occur. Consequently, these constants also affect the polarization resistance R_p.

As a final remark, it is important to point out that the high interface alkalination attained during Ni electrodeposition at pH 6 may give rise to a precipitation of hydroxide compounds at the electrode surface.[1] The presence of these products would reduce the available surface area and could also introduce some additional kinetic reactions. These difficulties would impair a satisfactory simulation of the experimental results at pH 6 by using the proposed model.

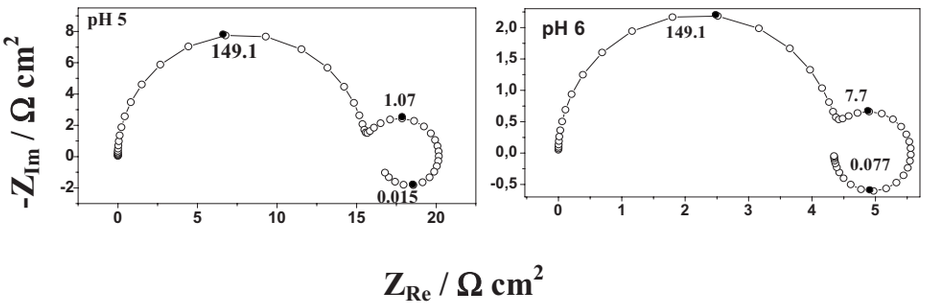

Figure 6. Simulated diagrams for 1.2 M $NiSO_4 \cdot 6H_2O$ solution, $E = -1.15$ V, at pH 5 and 6 (frequencies in hertz).

To summarize, the simulated results presented above show a satisfactory concordance with experimental data. The reaction model implies that the compounds $[Ni(OH)]^+_{ads}$ and $[Ni(OH)]_{ads}$ are involved in Ni electrodeposition within the pH range of 4–6. The species $[Ni(OH)]^+_{ads}$, associated with the capacitive loop at medium frequencies, is gradually consumed, being converted to $[Ni(OH)]_{ads}$, which becomes the main species at the potential domain related to part 2 of the polarization curves.

Conclusion

A kinetic model has been developed to account for the mechanism of Ni electrodeposition from acidic sulfate electrolytes over a pH range of 4–6. The model validation was done by the comparison with the experimental data obtained from steady-state polarization curves and impedance measurements.[1] The existence of two faradaic loops in the impedance diagrams allows the consideration of two adsorbed species at the electrode surface. The $\partial\theta_1/\partial E$ originates the capacitive loop at medium frequencies and is related to $[Ni(OH)]^+_{ads}$ species. The inductive loop is generated by $\partial\theta_2/\partial E$ and corresponds to the $[Ni(OH)]_{ads}$ adsorbed species.

The simulation of the pH increase was carried out by increasing k_{-4} and k_{-2} that govern the polarization resistance in the impedance plots. The reaction model was able to describe most experimental results: the pH and potentials effects on both the steady-state polarization curves and impedance diagrams. This model complements the previous one proposed[2] for pH values lower than 3. Consequently, a model for Ni electrodeposition in sulfate acid solutions in a broader pH interval, 1–6, would be useful in further investigations such as the mechanisms of Ni alloy electrodeposition.

Acknowledgments

The authors are grateful to the Brazilian agencies: Conselho Nacional de Desenvolvimento Científico e Tecnológico, Fundação de Amparo à Pesquisa do Estado do Rio de Janeiro, Coordenação de Aperfeiçoamento de Pessoal de Nível Superior, Financiadora de Estudos e Projetos, and Fundação Universitária José Bonifácio for their support.

Universidade Federal do Rio de Janeiro assisted in meeting the publication costs of this article.

References

1. A. I. C. Santana, S. L. Díaz, O. E. Barcia, and O. R. Mattos, *J. Electrochem. Soc.*, **156**, D326 (2009).
2. I. Epelboin, M. Jousselin, and R. Wiart, *J. Electroanal. Chem.*, **119**, 61 (1981).
3. I. Epelboin, M. Ksouri, and R. Wiart, *J. Electroanal. Chem.*, **65**, 373 (1975).
4. R. Wiart, *Electrochim. Acta*, **35**, 1587 (1990).
5. C. Cachet, I. Epelboin, M. Keddam, and R. Wiart, *J. Electroanal. Chem.*, **100**, 745 (1979).
6. E. Chassaing, M. Jousselin, and R. Wiart, *J. Electroanal. Chem.*, **157**, 75 (1983).
7. M. Keddam, O. R. Mattos, and H. Takenouti, *J. Electrochem. Soc.*, **128**, 257 (1981).
8. M. Keddam, O. R. Mattos, and H. Takenouti, *J. Electrochem. Soc.*, **128**, 266 (1981).
9. M. E. Orazem and B. Tribollet, *Electrochemical Impedance Spectroscopy*, p. 163, John Wiley & Sons, New York (2008).